Research Paper

Conformationally Strained *trans*-Cyclooctene (sTCO) Enables the Rapid Construction of ^{18}F-PET Probes via Tetrazine Ligation

Mengzhe Wang[1], Dennis Svatunek[2,3], Katarina Rohlfing[2], Yu Liu[2], Hui Wang[1], Ben Giglio[1], Hong Yuan[1], Zhanghong Wu[1], Zibo Li[1✉], and Joseph Fox[2✉]

1. Department of Radiology and Biomedical Research Imaging Center, University of North Carolina at Chapel Hill, Chapel Hill, North Carolina, 27599, United States.
2. Brown Laboratories, Department of Chemistry and Biochemistry, University of Delaware, Newark, Delaware 19716, United States.
3. Institute of Applied Synthetic Chemistry, TU Wien, Vienna, 1060, Austria.

✉ Corresponding authors: Zibo Li, PhD. Email: ziboli@med.unc.edu Phone: 919-962-5152 Fox, PhD. Email: jmfox@udel.edu Phone: 302-831-0191.

Abstract

The bioorthogonal reaction between tetrazines and *trans*-cyclooctenes is a method for the rapid construction of F-18 probes for PET imaging. Described here is a second generation ^{18}F-labeling system based on a conformationally strained *trans*-cyclooctene (sTCO)—a dienophile that is approximately 2 orders of magnitude more reactive than conventional TCO dienophiles. Starting from a readily prepared tosylate precursor, an ^{18}F labeled sTCO derivative (^{18}F-sTCO) could be synthesized in 29.3 +/- 5.1% isolated yield and with high specific activity. Tetrazine ligation was carried out with a cyclic RGD-conjugate of a diphenyl-*s*-tetrazine analogue (RGD-Tz) chosen from a diene class with an excellent combination of fast reactivity and stability both for the diene as well as the Diels-Alder adduct. For both the tetrazine and the sTCO, mini-PEG spacers were included to enhance solubility and improve the *in vivo* distribution profile of the resulting probe. Extremely fast reactivity (up to 2.86×10^5 $M^{-1}s^{-1}$ at 25 °C in water) has been observed in kinetic studies in the reaction of sTCO with diphenyl-*s*-tetrazine derivatives. A kinetic study on sTCO diastereomers in 55:45 MeOH:water showed that the *syn*-diastereomer displayed slightly faster reactivity than the *anti*-diastereomer. An ^{18}F-sTCO conjugate with RGD-Tz demonstrated prominent and persistent tumor uptake *in vivo* with good tumor-to-background contrast. Unlike most radiolabeled RGD peptides, the tumor uptake of this PET agent increased from 5.3 +/- 0.2% ID/g at 1 h post injection (p.i.), to 8.9 +/- 0.5% ID/g at 4 h p.i., providing evidence for prolonged blood circulation. These findings suggest that tetrazine ligations employing ^{18}F-sTCO should serve as a powerful and general platform for the rapid construction of peptide or protein derived PET agents.

Key words: bioorthogonal reaction, strained trans-cyclooctene (sTCO), positron emission tomography (PET), ^{18}F, RGD peptide.

Introduction

Positron emission tomography (PET) is a non-invasive imaging modality with the capacity to track radiolabeled biomolecules *in vivo*. This imaging technique employs radionuclides that emit positrons that collide with electrons and result in two detectable γ-rays.[1, 2] Of the common radionuclides that are utilized in PET, F-18 is the most broadly utilized due to the high positron efficiency, high specific radioactivity and clinically attractive half-life (~110 min).[3] These properties can minimize the toxic effects and radiation exposure to the patient. However, the short half-life of F-18, the modest nucleophilicity of fluoride, and the low concentrations that are intrinsic to both biology and radiochemistry

render it challenging to incorporate F-18 in complex biomolecules. The simple relationship between biomolecular rate constant and concentration shown in Table 1 illustrates the importance of fast rates to the field of F-18 labeling. Accordingly, there is a high demand for methods that efficiently introduce F-18 to biological macromolecules.

Table 1. Illustration of the practical importance of fast, bimolecular reactivity for radiolabeling at 1 μM. Radionuclides such as F-18 are prepared in small quantity and low concentration (typically ≤ 1 μM). Proteins and other biological macromolecules are typically utilized at micromolar concentrations. As both reactants are present in low concentration, fast reaction rates are essential to efficient coupling. The bioorthogonality and fast rate of the tetrazine-TCO ligation make it unusually well suited for radiolabeling applications.
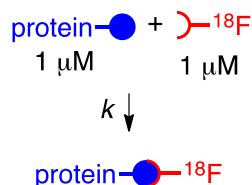
k (L/M·s)	$t_{1/2}$
10^6	1 sec
10^4	1.7 min
10^2	2.8 h
1	12 days
10^{-2}	3 years

The field of bioorthogonal chemistry is having a transformative influence on diverse fields including chemical biology, materials science, and nuclear medicine.[4-12] Since it was first introduced by us and others in 2008,[13-15] the tetrazine ligation has had a growing impact in biomedical research including radiolabeling, pretargeted imaging, *in vivo* reactions and other applications.[16-22] Our group has shown that the bioorthogonal reactions of tetrazines with *trans*-cyclooctene dienophiles proceed with exceptionally fast reaction rates (Figure 1).[23] The tetrazine-*trans*-cyclooctene ligation has become an important tool for biomolecular labeling because it is more rapid than other classes of bioorthogonal reactions.[24] Especially rapid reactivity has been observed for the conformationally strained dienophile, (1R,8S,E)-bicyclo[6.1.0]non-4-en-9-ylmethanol (sTCO),[25] for which rate constants as fast as 3.3 x 10^6 M^{-1}s^{-1} have been measured (Figure 1c).[26] By comparison, strain driven reactions of azides with cyclooctynes typically proceed with rates constants < 1 M^{-1}s^{-1}.[24] Speed of labeling is a premium consideration for radiolabeling biological molecules, as both the radiolabel and the biomolecule are typically low in concentration. Recently, intracellular labeling of HaloTag fusion proteins has been used to compare the efficiency of bioorthogonal reactions involving tetrazine or azides with cyclopropenes,

norbornenes, cycloalkenes and *trans*-cycloalkenes[10] In these studies, *trans*-cycloalkenes were identified as unique labeling reagents with sTCO-based reagents displaying the fastest reactivity. Moreover, while fluorescent reporters based on bicyclononyne (BCN) were prone to off-target labeling, TCO-based reporters were much more selective.[10] To date, radiolabeled analogs of sTCO have not yet been described.
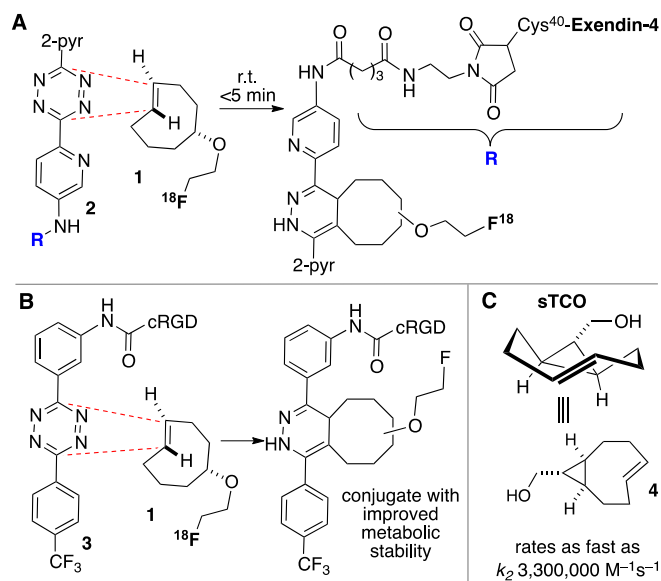
Figure 1. The tetrazine ligation with *trans*-cyclooctenes serves as a rapid method for the assembly of biomolecular-probe constructs. (A) The first generation system for F-18 labeling proceeds with fast kinetics but the Diels-Alder conjugate displays poor metabolic stability. (B) Diels-Alder conjugate from **1** and diphenyl-*s*-tetrazine derivative **3** displays improved metabolic stability. (C) The conformationally strained sTCO is the most reactive dienophile described to date, with rate constants of up to 3.3. x 10^6 M^{-1}s^{-1} for room temperature conjugations in water.

In recent years several radiolabeled *trans*-cyclooctenes and *s*-tetrazines have been developed for applications in rapid radiolabeling. Previously we described an F-18 radiolabeling method that utilizes functionalized derivatives of di-2-pyridyl-*s*-tetrazine (**2**) and an ^{18}F-labeled *trans*-cyclooctene (**1**) (Figure 1a).[23, 27-30] Analogs of these compounds have been shown to combine with rapid kinetics,[26] thereby enabling probe construction for cancer imaging and diabetes monitoring within seconds.[28, 30] More recently, we have explored the probe **3** derived from diphenyl-*s*-tetrazine, which is less rapid but gives Diels-Alder adducts with improved *in vivo* stability relative to the first generation system.[29] ^{18}F-labeled trans-cyclooctene **1** has also been investigated for pretargeted PET imaging in the brain.[31]

To great effect, Robillard and coworkers have used the *trans*-cyclooctene/di-2-pyridyl-*s*-tetrazine system for pretargeted cancer imaging. In this case *trans*-cyclooctene was used as a tagging compound

while a DOTA modified tetrazine moiety was used to attach either ^{111}In or ^{177}Lu radiolabels.[20, 21, 32-34] Weissleder and coworkers have shown that polymer modified tetrazines can be used for *in vivo* bioorthogonal labeling and PET imaging using ^{18}F-labeled TCO **1**.[17] Weissleder, Lewis and coworkers reported a pretargeting approach for PET imaging based on this method and demonstrated dramatically reduced non-targeted organ uptake.[22] Spivey and coworkers used a ^{68}Ga-DOTA modified 3-methyl-6-phenyl-*s*-tetrazine to construct probes from norbornene-labeled compounds.[35] In 2014, Devaraj and coworkers demonstrated that tetrazine modified, [64]Ga-chelating polymers could be employed in a proof-of-principle experiment for pretargeted PET imaging of *trans*-cyclooctene tagged antibodies targeting cancer cells.[36] Zeglis et al. used tetrazine bearing amino acids for [89]Zr labeling of peptides applying a *trans*-cyclooctene which was modified with deferrioxamine, a chelating agent for zirconium.[37]

While **1** was the only known ^{18}F labeled *trans*-cyclooctene, there have been considerable efforts recently to produce ^{18}F-labeled tetrazines. In 2014, Kuntner, Mikula and coworkers described a practical synthesis of an ^{18}F-labeled *s*-tetrazine.[38] While this dialkyl-*s*-tetrazine showed lower reactivity than commonly used tetrazines, direct F-18 labeling was possible and the compound exhibit good pharmacokinetic properties as well as high *in vivo* stability.[38] More recently, an ^{18}F-labeled 3-chloro-6-benzyloxy-s-tetrazine was described,[39] and Weissleder, Ploegh and coworkers introduced an ^{18}F labeled tetrazine based on ^{18}F-2-deoxyfluoroglucose, linked to a methyl-phenyl-s-tetrazine by oxime ligation, which enabled rapid radiolabeling of a trans-cyclooctene labeled peptide.[40] Ploegh, Liang and coworkers also introduced an ^{18}F labeled SFB-tetrazine and successfully construct PET probes with *trans*-cyclooctene tagged antibody fragment.[41] Lewis and coworkers introduced another ^{18}F-tetrazine in 2015, which was radiolabeled by an aluminum-[^{18}F]fluoride-NOTA-complex and successfully applied in pretargeted PET imaging of pancreatic cancer xenografts using a *trans*-cyclooctene labeled antibody.[42] A dipyridyl-*s*-tetrazine labeled by ^{11}C was recently introduced by Herth and coworkers.[43]

While there has been a surge in recent activity directed toward the development of new ^{18}F-labeled tetrazines, we recognized that the fastest reactivity would be borne out with conformationally strained sTCO derivatives. Accordingly, we sought to develop an ^{18}F labeled *trans*-cyclooctene that would display superior kinetics in tetrazine ligation. Here, we describe ^{18}F-sTCO—a new radiotracer based on the

most reactive trans-cyclooctene dienophile. It is shown that ^{18}F-sTCO rapidly combines with tetrazines and can be used to rapidly assemble probes for PET imaging. The kinetics in Diels-Alder reactions of the two diastereomers of sTCO were evaluated, and the more reactive *syn*-sTCO diastereomer was utilized for further study in PET probe construction. The tetrazine ligation with ^{18}F-sTCO was used to synthesize a radiolabeled RGD peptide and in a mouse tumor model was demonstrated to have a high level of tumor uptake relative to that in liver, kidney, and muscles. After 4 h post injection, the tumor was the most prominent image in the PET scan with tumor uptake that was 1.6–2.4 fold higher than other major organs.

Materials and methods

All commercially available analytical grade chemical reagents were purchased from Aldrich (St. Louis, MO) and used without further purification. Analytical reversed-phase HPLC using a Gemini 5μ C18 column (250 x 4.6mm) was performed on a SPD-M30A photodiode array detector (Shimadzu) and model 105S single-channel radiation detector (Carroll & Ramsey Associates). Radio HPLC analyses were carried out at 1 mL/min with water/acetonitrile eluent mixtures. For other HPLC analyses, the solvents were modified with 0.1% TFA.

Chemistry

Synthetic protocols, characterization details, and copies of ^{1}H NMR, ^{13}C NMR, and ^{19}F NMR spectra, the crude HPLC trace for ^{18}F labeling, and the HPLC data for the PBS stability study can be found in the Supplementary Material.

Stopped-Flow Kinetic Analysis

The second order rate constant was measured under pseudo-first order conditions using an excess of the appropriate sTCO diastereomer (**4** or **5**), and by following the exponential decay of absorbance due to the tetrazine chromophore of **11** at 298 nm using an SX 18MV-R stopped-flow spectrophotometer (Applied Photophysics Ltd.). For each run, equal volumes of 45:55 water:methanol solutions of sTCO and PEGylated tetrazine **11** were mixed in the stopped flow device. Reactions were carried out with tetrazine **11** at 0.05 mM and final concentrations of 0.245, 0.49, 0.98 and 1.47 mM for the *syn*-diastereomer **5**. Similarly, reactions were carried out with tetrazine **11** at 0.05 mM and final concentrations of 0.25, 0.50, 1.00 and 1.50 mM for the *anti*-diastereomer **4**. A total of 400 data points were recorded over a period of 1 second, and each sample was performed in sextuplicate at 298 K. The k_{obs} was determined by

nonlinear regression analysis of the data points using Prism software (v. 6.00, GraphPad Software Inc.). The results are reported in the Supporting Information.

Radiochemistry

The radiolabeling reactions were carried out using the following protocol unless specified. sTCO-tosylate **8** (9.1 µmol) was dissolved in MeCN (30 µL) and then allowed to react with ^{18}F-TBAF (200 mCi) at 85 °C for 10 min. The reaction was quenched by adding water (500 µL). The mixture was then passed through a Sep-Pak cartridge (Sep-Pak Plus light alumina) followed by HPLC purification. After HPLC purification, the fraction containing the desired product was diluted with 10 mL of water, trapped on C18 Sep-Pak, washed with 10 mL water, and eluted off with 0.5 mL EtOH. A portion of the solution containing [18]**F-9** was reserved for the *in vitro* stability test. Then a fraction of the solution (10 mCi, estimated to be 4.8 nmol) was mixed with a DMSO solution of tetrazine-RGD conjugate **12** (ranging from 0.07 µmol to 3.3 nmol). After shaking for 10 seconds at room temperature, a portion of the reaction mixture (3 mCi) was loaded onto HPLC for further analysis. The HPLC eluent containing [18]**F-15** was collected and organic solvent was removed using rotary evaporator. After carefully adjusting the pH to 7.5, [18]**F-15** was reconstituted in 1x PBS for the stability test and small animal studies.

In Vitro Stability

[18]**F-9** and [18]**F-15** was incubated in 1x PBS buffer at 37 °C. An aliquot of the solution (~25 µCi) was taken out and loaded on HPLC at 1 h and 2 h time point for analysis. [18]**F-9** was also incubated in FBS at 37 °C and after 1 h, an aliquot of the solution (~25 µCi) was taken out and added to an equal volume of TFA. Similarly, [18]**F-15** was also incubated in FBS at 37 °C, and at 2 and 4 h time points, aliquots of the solution (~25 µCi) were taken and added to an equal volume of TFA. For each sample, the mixture was centrifuged at 14000 rpm for 5 min. The supernatant was then diluted with 1 mL water and loaded on C18 Sep-Pak. After washing with 1 mL water, the cartridge was eluted with 0.5 mL acetonitrile. The water fraction and acetonitrile fraction were combined and loaded on HPLC for analysis

Small Animal PET Imaging

Animal procedures were performed according to a protocol approved by the UNC Institutional Animal Care and Use Committee. PET scans and image analysis were performed using a small animal PET scanner as previously reported.[44] Human U87MG tumor-bearing mice were anesthetized using 2% isoflurane and injected with 3.7 MBq (100 µCi) of [18]**F-15** via the tail vein. At 0.5, 1.0, 2.0, and 4.0 h post injection, static emission scans were acquired for 10 min. Normal nude mice were injected with 3.7 MBq (100 µCi) of ^{18}F-sTCO-PEG-tetrazine (compound obtained by combining [18]**F-9** and **11**) or [18]**F-9** using the same protocol. Raw PET images were reconstructed using 2D ordered subset expectation maximization (OSEM) algorithm. No background correction was performed. Regions of interest (ROI) were manually drawn over the tumor and other organs on the decay corrected coronal images. Based on the assumption that the tissue density is 1 g/mL, the ROIs were converted to % ID/g by dividing dose per gram at ROI by injected dose.

Statistical analysis

Quantitative data were expressed as mean ± SD. Means were compared using one-way ANOVA and Student's t test. *P* values <0.05 were considered statistically significant.

Results and Discussion

Chemistry

The *anti*-diastereomer of sTCO (**4**) was prepared as described previously, and the *syn*-diastereomer **5** was prepared as shown in Figure 2A. Thus, photoisomerization of **7** using our previously described flow reactor [14] gave *syn*-sTCO **5** in 81% yield. Our initial efforts to activate *syn*-sTCO **5** through reaction with NsCl or TsCl were unsuccessful, and lead only to skeletal rearrangement products. After
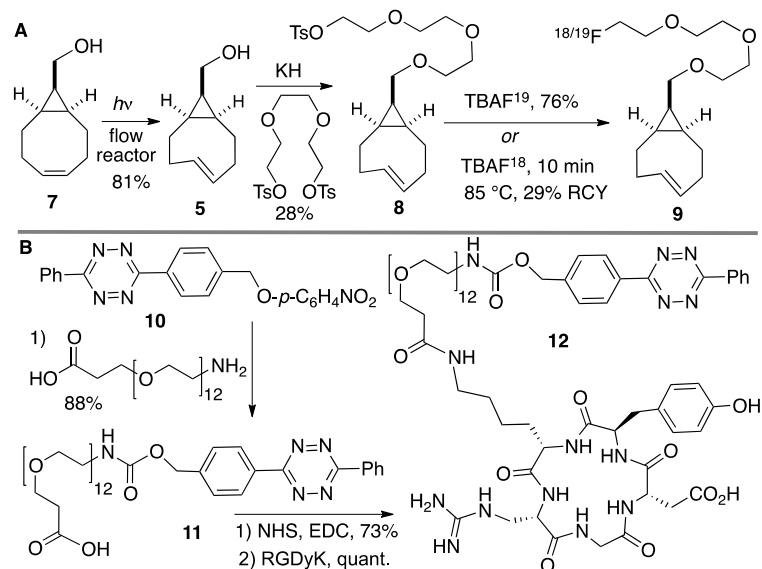
Figure 2. (A) Synthesis of *syn*-sTCO **5**, labeling precursor **8**, cold standard [19]**F-9**, and radiotracer [18]**F-9**. (B) Synthesis of a cyclic RGD-diphenyl-*s*-tetrazine conjugate **12**.

experimentation, we developed a synthesis that directly provided a tosylate product through alkylation of the alcohol **5** with a bis-tosylate that contained a mini-PEG linker. Thus, combination of this alcohol with KH and triethylene glycol ditosylate gave the sTCO tosylate **8** in 28% yield. To create the HPLC standard, the treatment of **8** with TBAF in anhydrous THF gave the ^{19}F-labeled derivative **9** in 76% yield. A diphenyl-*s*-tetrazine conjugate of a cyclic RGD was synthesized as shown Figure 2B. The nitrophenylcarbonate **10** was sequentially coupled with a "mini-PEG" amino acid to give **11**. Subsequent coupling with NHS and conjugation with the cyclic peptide RGDyK gave **12** in high yield.
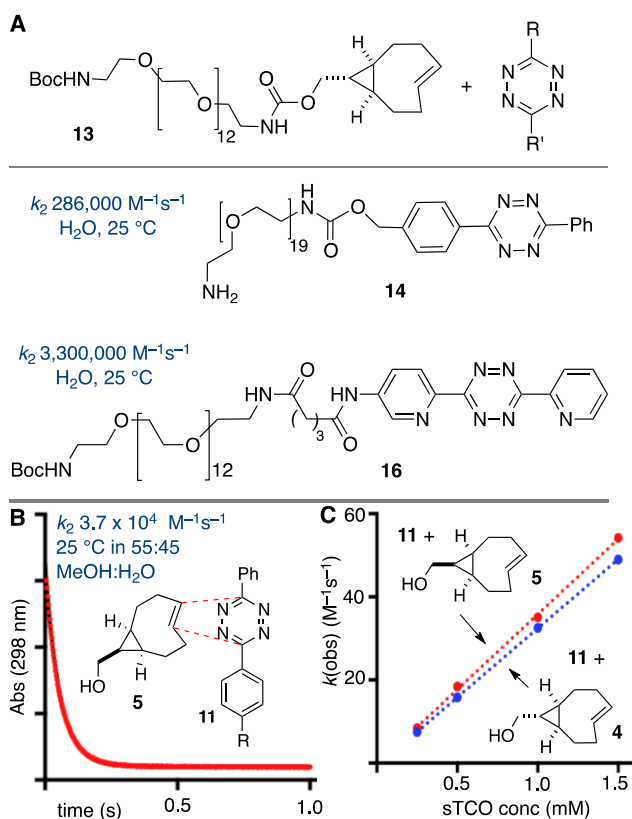
Figure 3. Rapid reactions of s-TCO derivatives with tetrazines. (A) Rate constants of *anti*-sTCO and tetrazine analogs in water. (B,C) Rate constants for the *syn*- and *anti*-diastereomers of sTCO were measured in mixed aqueous/organic media. (B) Kinetic data for the reaction of **5** (0.49 mM) and **11** (0.05 mM). The sTCO *syn*-diastereomer **5** is slightly more reactive than the *anti*-diastereomer **4**.

Stopped flow kinetic analysis was used to measure the rate of the Diels-Alder reaction between tetrazine derivative **11** and *anti*- and *syn*-diastereomers of sTCO (**4** and **5**, respectively). In a prior study with **13**, a mini-PEG derivative of the sTCO *anti*-diastereomer, it was found that the water soluble diphenyl-*s*-tetrazine analog **14** and the di-2-pyridyl-*s*-tetrazine analog **16** react with rate constants of 2.86×10^5 M^{-1}s^{-1} and 3.3×10^6 M^{-1}s^{-1} (Figure 3a). The latter is the fastest rate constant that

has been described for a bioorthogonal reaction. For the present study, we used stopped flow analysis to compare the relative rate of the *syn*- and *anti*-diastereomers of sTCO with tetrazine **11** in mixed organic/aqueous media (55:45 MeOH:water at 25 °C). As expected, the rates in MeOH:water were ~9 fold slower than the measurements made in purely aqueous media, but still extremely rapid. The rate constant for the *syn*-diastereomer **5** with tetrazine **11** was k_2 3.7×10^4 (+/− 0.1×10^3) M^{-1}s^{-1}, and the *anti*-diastereomer **4** reacted with a rate constant k_2 3.3×10^4 (+/− 0.1×10^3) M^{-1}s^{-1}. Because the *syn*-diastereomer was more reactive it was chosen for further development in PET probe construction.

Radiochemistry

[18]F-labeled sTCO ([18]**F-9**) was produced using the protocol described in Figure 2. By treating tosylate precursor **8** (182 mM) with ^{18}F-TBAF in acetonitrile at 85 °C for 10 min, we were able to obtain the radiolabeled [18]**F-9** in 29.3 +/− 5.1% isolated radiochemical yield with 99% radiochemical purity after HPLC purification (Figure 2a, Figure 5a). Here, the reaction concentration was determined to be important, as running the reaction at 91 mM gave [18]**F-9** in only 9.3 +/− 2.4% isolated yield. The specific activity was determined to be 2.1 +/- 0.8 Ci/µmol. The product identity was confirmed by co-injection with an independently synthesized [19]**F-9** standard. Prior to reacting with targeting molecules, we first tested the *in vitro* stability of [18]**F-9**. After incubation in 1X PBS, the radiopurity remained at 97.5% and 97.3% at 1 hour and 2 hour time points, respectively (Figure S3). This result demonstrated that [18]**F-9** is sufficiently stable to construct PET probes in aqueous solution. It was also observed that [18]**F-9** was stable in fetal bovine serum for 1 hour with retention of 74% radiochemical purity (Figure S10).

As depicted in Figure 4, the conjugation of [18]**F-9** with RGD-tetrazine **12** (700 µM) produced conjugate [18]**F-15** as a mixture of isomers. The starting material [18]**F-9** was completely consumed upon initial assay (<5 minutes). Reducing the concentration of **12** to 33 µM lead to an inversion in stoichiometry, and the complete consumption of **12** and the observation of unreacted [18]**F-9**. This ability to achieve complete labeling when the ^{18}F-labeled substrate is used *in excess* speaks to the high efficiency and rate of bioorthgonal reaction using [18]**F-9**.

Under ambient reaction conditions, a 91% radiochemical yield of [18]**F-15** was obtained with 99% purity (Figure S4) after HPLC purification. The crude radio-HPLC trace is displayed in Figure 5B. The specific activity was determined to be 0.91 +/- 0.20 Ci/µmol. An analog reaction with [19]**F-9** produced the

isomeric "cold" Diels-Alder conjugates **¹⁹F-15**. LC-MS analysis confirmed that the both of the major peaks from the conjugation had mass spectra matching the theoretical for **¹⁹F-15** (Supporting Information). More rapidly eluting minor peaks also had correct mass data, and likely correspond to the aminal (hydrated) forms of the product.[25] The slowest eluting peak from the radio-HPLC trace of **¹⁸F-15** was collected and the *in vitro* stability was studied. It was observed that the adduct was stable in PBS buffer for 2 hours with retention of 98.5% radiochemical purity (Figure 5C). Conjugate **¹⁸F-15** was also found to be stable in fetal bovine serum with 96.7% and 94.5% purity at 2 and 4 hours post incubation respectively. (Figure S10)
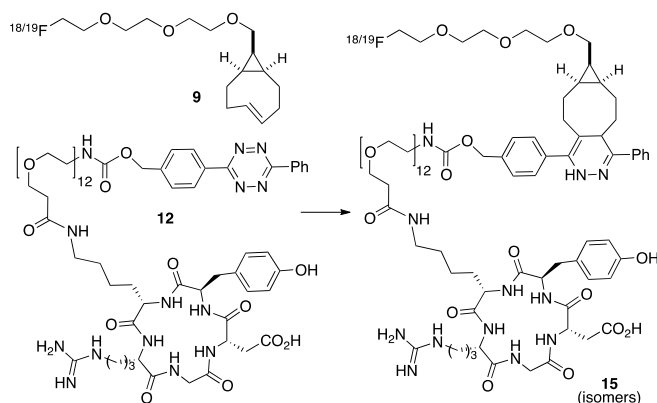

Figure 4. Conjugation of **¹⁸F-9** with RGD-tetrazine **12** to produce conjugate **¹⁸F-15** as a mixture of isomers. Cold standards were independently prepared.

Due to the low concentration and short time scale that is intrinsic to ¹⁸F labeling of proteins, the fast kinetics and bioorthogonality of the tetrazine-TCO ligation provide a clear benefit over conventional radiolabeling methods. With our prior system, highly reactive tetrazines were required in order to obtain rapid reactivity at micromolar concentrations, but the resulting Diels-Alder conjugates had only moderate stability *in vivo* (Figure 1a).[30] The superior reactivity of ¹⁸F-sTCO allows rapid kinetics ($>10^4$ M⁻¹s⁻¹) to be realized with more stable diphenyl-*s*-tetrazines, giving rise to Diels-Alder conjugates which are known to possess improved *in vivo* stability.[29] Moreover, the system described here leads to conjugates with improved blood circulation and higher levels of tumor uptake than observed using the previously described systems shown in Figure 1.

Small Animal PET imaging

The localization of **¹⁸F-15** in human U87MG tumor-bearing mice (n=5) was performed by static microPET scans at multiple time-point post tail vein injection. Selected decay-corrected coronal images at different time points are shown in Figure 6 after injection of 3.7 MBq (100 µCi) of **¹⁸F-15**. High and

persistent tumor accumulation was observed with good tumor to background contrast as early as 30 min post injection. The 2D maximum intensity projection for the images displayed in Figure 6 and S9. The quantitative biodistribution derived from small-animal PET images are shown in Figure 7. The inclusion of mini-PEG spacers resulted in a biodistribution profile that was significantly improved relative to previously constructed TCO/tetrazine-based probes that lack a PEG spacer, and the blood circulation of this new construct was improved significantly compared with previously described constructs. The tumor uptake was 5.3 +/- 0.2, 6.9 +/- 0.5, 7.5 +/- 0.8 and 8.9 +/- 0.5 % ID/g at 0.5, 1.0, 2.0, and 4.0 h post injection, respectively. At 4.0 h post injection, the tumor became the brightest spot in PET scan, with a tumor-to-liver and tumor-to-kidney ratio of 1.6 and 2.4, respectively. Given the improved blood circulation and high levels of tumor uptake for this small peptide-based probe, we anticipate that ¹⁸F-sTCO based probes should find broad utility for the labeling of larger peptides, proteins and other biomolecules.
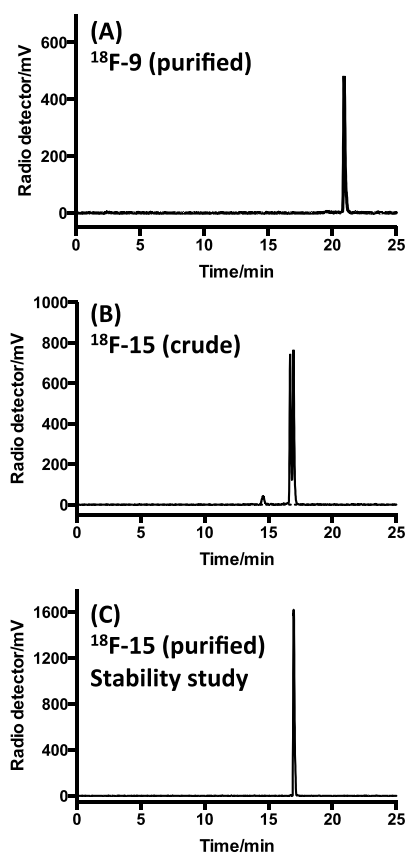
**Figure 5.** Radio-HPLC analyses. (A) Purified **¹⁸F-9** after incubation in PBS for 2 h at 37 °C. (B) Combination of **¹⁸F-9** with **12** gives two major isomeric adducts **¹⁸F-15**. (C) The slow eluting isomer of **¹⁸F-15** after purified by HPLC, incubation in PBS for 2 h at 37 °C, and reanalysis.

The specificity of [18]F-15 was confirmed by a blocking experiment in which the radiotracer was co-injected with an excess amount of cRGDyK. The RGD peptide is a well-established targeting molecule,[45-49] and as can be seen in Figure 6B, in the presence of non-radio labeled cRGDyK (200 µg), the tracer uptake in tumor dropped to 4.8 +/- 0.3% at 1 h post injection. As expected the cRGDyK peptide, which should be readily cleared than a PEGylated peptide, did not completely block the signal due to [19]F-15. However, the signal in the presence of blocking cRGDyK was significantly (P<0.05) lower than that observed without a blocking agent.

We also performed microPET imaging with a normal (non-tumor bearing) nude mouse that had been injected with [18]F-9. The imaging data indicated that the compound was rapidly cleared by the gallbladder, kidney and liver within 2 hours (Figure S8). We also analyzed the clearance of the compound obtained by combining [18]F-9 with 11. This Diels-Alder conjugate— an analog of [18]F-15 that lacks the RGD moiety— still remained in the blood circulatory system after 4 hours (Figure S7). The blood uptake was 2.4% ID/g at 4 h post injection. Previously, we have described ^{18}F-labeled RGD probes derived from *trans*-cyclooctene **1** (Figure 1). These probes which lack PEGylation are cleared much more rapidly.[29, 30] These results suggested that the entire PEGylated Diels-Alder moiety plays a role in enhancing the circulation time of the probe. Future experiments will aim to determine the respective contributions of the Diels-Alder conjugate and the PEG chains as factors in increasing the circulation lifetime. We believe that the rapid clearance of [19]F–9 and the long circulation lifetime of its PEGylated Diels-Alder conjugates may prove advantageous for future applications in pretargeted imaging, and we are currently pursuing these applications.
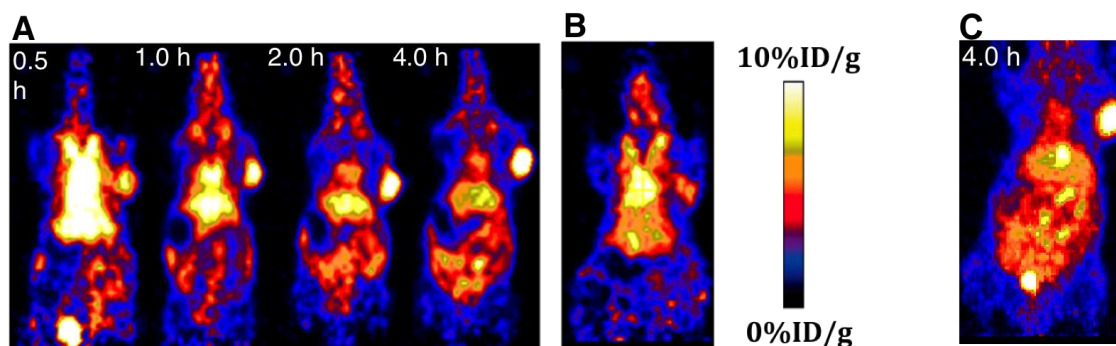
Figure 6. (A) Small animal PET images of mice bearing U87 xenograft, injected with [18]F-15 and imaged 0.5 h, 1.0 h, 2.0 h and 4.0 h post injection, respectively. (B) A 'blocking' experiment in which cyclic RGDyK peptide (200 µg) was injected prior to the injection of [18]F-15, with imaging at 1.0 h post injection. (C) Two-dimensional maximum intensity projection at 4.0 h post injection of [18]F-15.
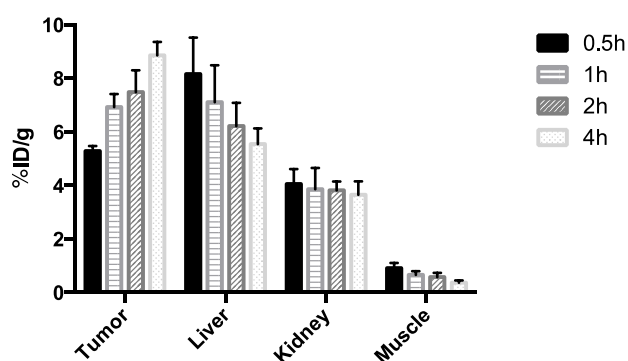
Figure 7. Tumor and major organ radioactivity accumulation quantification from a static scan at 0.5, 1, 2, and 4 h post injection of [18]F-15 into U87MG tumor model. Data are expressed as average +/- SD.

Conclusions

A conformationally strained trans-cyclooctene, ^{18}F-sTCO (**9**), was prepared via a one-step fluorination. This new PET-tracer is based on the conformationally strained *trans*-cyclooctene (sTCO)—a dienophile that is approximately 2 orders of magnitude more reactive than conventional TCO dienophiles. In a model system, the rate constants for sTCO-diastereomers were compared, and the *syn*-diastereomer was found to be slightly more reactive and therefore was chosen for further development. The effectiveness of 9 for the construction of radiolabeled probes was demonstrated with the production of a cyclic RGD based probe **15**. Mini-PEG groups were included in the design of **15** to improve both the water solubility and the pharmacokinetic properties of the probe. In tumor-bearing mice, [18]F-**15** demonstrated a significantly improved blood half-life compared with monomeric RGD peptide analogs. As a result, increased tumor uptake of [18]F-**15** was observed at a late time point. Given the exceptional kinetics of [18]F-**9** and the improved tumor uptake and accumulation of the derived probe [18]F-**15**, we expect that this labeling system will be broadly applicable for attachment of F-18 to a host of applications in probe construction,

pretargeted imaging, and treatment applications.

Supplementary Material

Acknowledgment

Competing Interests

The authors have declared that no competing interest exists.

References

1. Sorensen J. How Does the Patient Benefit from Clinical PET? Theranostics. 2012; 2: 427-36.
2. Schlyer DJ. PET tracers and radiochemistry. Ann Acad Med Singapore. 2004; 33: 146-54.
3. Li Z, Conti PS. Radiopharmaceutical chemistry for positron emission tomography. Adv Drug Deliv Rev. 2010; 62: 1031-51.
4. Patterson DM, Prescher JA. Orthogonal bioorthogonal chemistries. Curr Opin Chem Biol. 2015; 28: 141-9.
5. King M, Wagner A. Developments in the field of bioorthogonal bond forming reactions-past and present trends. Bioconjug Chem. 2014; 25: 825-39.
6. McKay CS, Finn MG. Click chemistry in complex mixtures: bioorthogonal bioconjugation. Chem Biol. 2014; 21: 1075-101.
7. Patterson DM, Nazarova LA, Prescher JA. Finding the right (bioorthogonal) chemistry. ACS Chem Biol. 2014; 9: 592-605.
8. Kang SW, Lee S, Na JH, Yoon HI, Lee DE, Koo H, et al. Cell labeling and tracking method without distorted signals by phagocytosis of macrophages. Theranostics. 2014; 4: 420-31.
9. Fox JM, Robillard MS. Editorial overview: In vivo chemistry: Pushing the envelope. Curr Opin Chem Biol. 2014; 21: v-vii.
10. Murrey HE, Judkins JC, Am Ende CW, Ballard TE, Fang Y, Riccardi K, et al. Systematic Evaluation of Bioorthogonal Reactions in Live Cells with Clickable HaloTag Ligands: Implications for Intracellular Imaging. J Am Chem Soc. 2015; 137: 11461-75.
11. Zhang H, Dicker KT, Xu X, Jia X, Fox JM. Interfacial Bioorthogonal Cross-Linking. ACS Macro Lett. 2014; 3: 727-31.
12. Liu S, Zhang H, Remy RA, Deng F, Mackay ME, Fox JM, et al. Meter-long multiblock copolymer microfibers via interfacial bioorthogonal polymerization. Adv Mater. 2015; 27: 2783-90.
13. Blackman ML, Royzen M, Fox JM. The Tetrazine Ligation: Fast Bioconjugation based on Inverse-electron-demand Diels-Alder Reactivity. J Am Chem Soc. 2008; 130: 13518-9.
14. Royzen M, Yap GPA, Fox JM. A Photochemical Synthesis of Functionalized trans-Cyclooctenes Driven by Metal Complexation. J Am Chem Soc. 2008; 130: 3760-1.
15. Selvaraj R, Fox JM. trans-Cyclooctene—a stable, voracious dienophile for bioorthogonal labeling. Current Opinion in Chemical Biology. 2013; 17: 753-60.
16. Carroll L, Evans HL, Aboagye EO, Spivey AC. Bioorthogonal chemistry for pre-targeted molecular imaging - progress and prospects. Org Biomol Chem. 2013; 11: 5772-81.
17. Devaraj NK, Thurber GM, Keliher EJ, Marinelli B, Weissleder R. Reactive polymer enables efficient in vivo bioorthogonal chemistry. Proc Natl Acad Sci U S A. 2012; 109: 4762-7.
18. Devaraj NK, Upadhyay R, Haun JB, Hilderbrand SA, Weissleder R. Fast and Sensitive Pretargeted Labeling of Cancer Cells via Tetrazine/Trans-Cyclooctene Cycloaddition. Angew Chem Int Ed Engl. 2009; 48: 7013-6.
19. Reiner T, Zeglis BM. The inverse electron demand Diels-Alder click reaction in radiochemistry. J Labelled Comp Radiopharm. 2014; 57: 285-90.
20. Rossin R, Läppchen T, van den Bosch SM, Laforest R, Robillard MS. Diels-Alder Reaction for Tumor Pretargeting: In Vivo Chemistry Can Boost Tumor Radiation Dose Compared with Directly Labeled Antibody. J Nucl Med. 2013; 54: 1989-95.
21. Rossin R, Renart Verkerk P, van den Bosch SM, Vulders RCM, Verel I, Lub J, et al. In Vivo Chemistry for Pretargeted Tumor Imaging in Live Mice. Angew Chem Int Ed Engl. 2010; 49: 3375-8.
22. Zeglis BM, Sevak KK, Reiner T, Mohindra P, Carlin SD, Zanzonico P, et al. A Pretargeted PET Imaging Strategy Based on Bioorthogonal Diels-Alder Click Chemistry. J Nucl Med. 2013; 54: 1389-96.
23. Wu Z, Liu S, Hassink M, Nair I, Park R, Li L, et al. Development and Evaluation of ^{18}F-TTCO-Cys40-Exendin-4: A PET Probe for Imaging Transplanted Islets. J Nucl Med. 2013; 54 :244-51.
24. Lang K, Chin JW. Bioorthogonal Reactions for Labeling Proteins. ACS Chemical Biology. 2014; 9: 16-20.
25. Taylor MT, Blackman ML, Dmitrenko O, Fox JM. Design and synthesis of highly reactive dienophiles for the tetrazine-trans-cyclooctene ligation. J Am Chem Soc. 2011; 133: 9646-9.
26. Darko A, Wallace S, Dmitrenko O, Machovina MM, Mehl RA, Chin JW, et al. Conformationally Strained -Cyclooctene with Improved Stability and Excellent Reactivity in Tetrazine Ligation. Chem Sci. 2014; 5: 3770-6.
27. Li Z, Cai H, Hassink M, Blackman ML, Brown RCD, Conti PS, et al. Tetrazine-trans-cyclooctene ligation for the rapid construction of ^{18}F labeled probes. Chem Commun (Camb). 2010; 46: 8043-5.
28. Liu S, Hassink M, Selvaraj R, Yap L-P, Park R, Wang H, et al. Efficient ^{18}F labeling of cysteine containing peptides and proteins using the tetrazine-trans-cyclooctene ligation. Molecular imaging. 2013; 12: 121-8.
29. Selvaraj R, Giglio BC, Liu S, Wang H, Wang M, Yuan H, et al. Improved Metabolic Stability for ^{18}F PET Probes Rapidly Constructed via Tetrazine trans-Cyclooctene Ligation. Bioconjug Chem. 2015; 26: 435-42.
30. Selvaraj R, Liu S, Hassink M, Huang C-w, Yap L-p, Park R, et al. Tetrazine-tans-cyclooctene ligation for the rapid construction of integrin $\alpha_v\beta_3$ targeted PET tracer based on a cyclic RGD peptide. Bioorg Med Chem Lett 2011; 21: 5011-4.
31. Wyffels L, Thomae D, Waldron AM, Fissers J, Dedeurwaerdere S, Van der Veken P, et al. In vivo evaluation of ^{18}F-labeled TCO for pre-targeted PET imaging in the brain. Nucl Med Biol. 2014; 41: 513-23.
32. Rossin R, van den Bosch SM, Ten Hoeve W, Carvelli M, Versteegen RM, Lub J, et al. Highly reactive trans-cyclooctene tags with improved stability for Diels-Alder chemistry in living systems. Bioconjug Chem. 2013; 24: 1210-7.
33. Rossin R, van Duijnhoven SM, Lappchen T, van den Bosch SM, Robillard MS. Trans-cyclooctene tag with improved properties for tumor pretargeting with the diels-alder reaction. Mol Pharm. 2014; 11: 3090-6.
34. van Duijnhoven SM, Rossin R, van den Bosch SM, Wheatcroft MP, Hudson PJ, Robillard MS. Diabody Pretargeting with Click Chemistry In Vivo. J Nucl Med. 2015; 56: 1422-8.
35. Evans HL, Carroll L, Aboagye EO, Spivey AC. Bioorthogonal chemistry for ^{68}Ga radiolabelling of DOTA-containing compounds. J Labelled Comp Radiopharm. 2014; 57: 291-7.
36. Nichols B, Qin Z, Yang J, Vera DR, Devaraj NK. [68]Ga chelating bioorthogonal tetrazine polymers for the multistep labeling of cancer biomarkers. Chem Commun (Camb). 2014; 50: 5215-7.
37. Zeglis BM, Emmetiere F, Pillarsetty N, Weissleder R, Lewis JS, Reiner T. Building Blocks for the Construction of Bioorthogonally Reactive Peptides via Solid-Phase Peptide Synthesis. ChemistryOpen. 2014; 3: 48-53.
38. Denk C, Svatunek D, Filip T, Wanek T, Lumpi D, Frohlich J, et al. Development of a ^{18}F-labeled tetrazine with favorable pharmacokinetics for bioorthogonal PET imaging. Angew Chem Int Ed Engl. 2014; 53: 9655-9.
39. Zhu J, Li S, Wangler C, Wangler B, Lennox RB, Schirrmacher R. Synthesis of 3-chloro-6-((4-(di-tert-butyl[18]F]fluorosilyl)-benzyl)oxy)-1,2,4,5-tetrazine ([^{18}F]SiFA-OTz) for rapid tetrazine-based ^{18}F-radiolabeling. Chem Commun (Camb). 2015; 51: 12415-8.
40. Rashidian M, Keliher EJ, Dougan M, Juras PK, Cavallari M, Wojtkiewicz GR, et al. Use of ^{18}F-2-Fluorodeoxyglucose to Label Antibody Fragments for Immuno-Positron Emission Tomography of Pancreatic Cancer. ACS Central Science. 2015; 1: 142-7.
41. Rashidian M, Wang L, Eden JG, Jacobsen JT, Hossain I, Wang Q, et al. Enzyme-Mediated Modification of Single-Domain Antibodies for Imaging Modalities with Different Characteristics. Angewandte Chemie International Edition. 2015; 02142.
42. Meyer JP, Houghton JL, Kozlowski P, Abdel-Atti D, Reiner T, Pillarsetty NV, et al. F-Based Pretargeted PET Imaging Based on Bioorthogonal Diels-Alder Click Chemistry. Bioconjug Chem. 2015.
43. Herth MM, Andersen VL, Lehel S, Madsen J, Knudsen GM, Kristensen JL. Development of a ^{11}C-labeled tetrazine for rapid tetrazine-trans-cyclooctene ligation. Chem Commun (Camb). 2013; 49: 3805-7.
44. Deng H, Wang H, Wang M, Li Z, Wu Z. Synthesis and Evaluation of ^{64}Cu-DOTA-NT-Cy5.5 as a Dual-Modality PET/Fluorescence Probe to Image Neurotensin Receptor-Positive Tumor. Mol Pharm. 2015; 12: 3054-61.
45. Lang L LW, Jia HM, Fanng DC, Zhang S, Sun X, Zhu L, Ma Y, Shen B, Kieswetter DO, Niu G, Chen X. New Methods for Labeling RGD Peptides With Bormine-76. Theranostics. 2011; 1: 341-53.
46. Chen X, Park R, Shahinian AH, Tohme M, Khankaldyyan V, Bozorgzadeh MH, et al. 18F-labeled RGD peptide: Initial evaluation for imaging brain tumor angiogenesis. Nuclear Medicine and Biology. 2004; 31: 179-89.

47. Chen H, Niu G, Wu H, Chen X. Clinical Application of Radiolabeled RGD Peptides for PET Imaging of Integrin αvβ3. Theranostics. 2016; 6: 78-92.
48. Zhang Y, Yang Y, Cai W. Multimodality Imaging of Integrin α(v)β(3) Expression. Theranostics. 2011; 1: 135-48.
49. Ye Y, Chen X. Integrin targeting for tumor optical imaging. Theranostics. 2011; 1: 102-26.